The kinase TBK1 functions in dendritic cells to regulate T cell homeostasis, autoimmunity, and antitumor immunity

Yichuan Xiao,[1,3]* Qiang Zou,[2,3]* Xiaoping Xie,[3]* Ting Liu,[3,6] Haiyan S. Li,[3] Zuliang Jie,[3] Jin Jin,[3,7] Hongbo Hu,[3,6] Ganiraju Manyam,[5] Li Zhang,[5,8] Xuhong Cheng,[3] Hui Wang,[3] Isabelle Marie,[9,10,11] David E. Levy,[9] Stephanie S. Watowich,[3,4] and Shao-Cong Sun[3,4]

[1]Key Laboratory of Stem Cell Biology, Institute of Health Sciences, Shanghai Institutes for Biological Sciences, Chinese Academy of Sciences/Shanghai Jiao Tong University School of Medicine, Shanghai 200031, China
[2]Department of Immunology and Microbiology, Shanghai Institute of Immunology, Key Laboratory of Cell Differentiation and Apoptosis of Chinese Ministry of Education, Shanghai Jiao Tong University School of Medicine, Shanghai 200025, China
[3]Department of Immunology, MD Anderson Cancer Center, [4]Graduate School of Biomedical Sciences, and [5]Department of Bioinformatics and Computational Biology, MD Anderson Cancer Center, The University of Texas, Houston, TX 77030
[6]State Key Laboratory of Biotherapy, West China Hospital, Si-Chuan University and Collaborative Innovation Center for Biotherapy, Chengdu 610041, China
[7]Life Sciences Institute, Zhejiang University, Hangzhou 310058, China
[8]Department of Environmental Health, University of Cincinnati, Cincinnati, OH 45220
[9]Department of Pathology, [10]Department of Microbiology, and [11]NYU Cancer Institute, NYU School of Medicine, New York, NY 10016

Dendritic cells (DCs) are crucial for mediating immune responses but, when deregulated, also contribute to immunological disorders, such as autoimmunity. The molecular mechanism underlying the function of DCs is incompletely understood. In this study, we have identified TANK-binding kinase 1 (TBK1), a master innate immune kinase, as an important regulator of DC function. DC-specific deletion of *Tbk1* causes T cell activation and autoimmune symptoms and also enhances antitumor immunity in animal models of cancer immunotherapy. The TBK1-deficient DCs have up-regulated expression of co-stimulatory molecules and increased T cell–priming activity. We further demonstrate that TBK1 negatively regulates the induction of a subset of genes by type I interferon receptor (IFNAR). Deletion of IFNAR1 could largely prevent aberrant T cell activation and autoimmunity in DC-conditional *Tbk1* knockout mice. These findings identify a DC-specific function of TBK1 in the maintenance of immune homeostasis and tolerance.

INTRODUCTION

The immune system is capable of launching robust responses against invading pathogens while maintaining tolerance to self-antigens. As the primary antigen-presenting cells, DCs are crucial for both stimulating T cell responses to foreign antigens and maintaining immune tolerance to self-antigens (Steinman et al., 2003; Mayer et al., 2012; Hammer and Ma, 2013). Although the tolerant function of DCs is important for preventing autoimmune diseases, it also poses a major obstacle for immune responses against cancer, and a general principal of cancer immunotherapy is to break immune tolerance (Sharma et al., 2011; Maueröder et al., 2014). DCs sense the environment largely via pattern-recognition receptors (PRRs), which recognize diverse molecular patterns associated with pathogens and commensal microbes, as well as self-ligands such as DNAs released from dying cells (van Vliet et al., 2007; Seya et al., 2010; Ahn and Barber, 2014). During an infection, DCs are stimulated for maturation by pathogen-associated molecular patterns, acquiring the ability to stimulate T cells for immune activation (Dudek et al., 2013; Hammer and Ma, 2013). However, in steady state, DCs undergo partial or homeostatic maturation, characterized by low surface expression of co-stimulatory molecules (e.g., CD80 and CD86), which is important for maintaining peripheral immune tolerance by inducing T cell anergy and promoting regulatory T cell (T reg cell) production (Dhodapkar et al., 2001; Hawiger et al., 2001; Mahnke et al., 2002; Dalod et al., 2014). The signaling network that mediates the tolerant function of DCs has been poorly defined.

TANK-binding kinase 1 (TBK1) along with its homologue IκB kinase epsilon (IKKε; also known as IKKi) are innate immune kinases that activate the transcription factor IRF3 and, thereby, mediate induction of type I IFNs by various PRR ligands during viral infections (Fitzgerald et al., 2003; Sharma et al., 2003; Hemmi et al., 2004; McWhirter et al., 2004; Hiscott, 2007). TBK1 and IKKε display redundant or unique functions in IFN induction depending on the cell

*Y. Xiao, Q. Zou, and X. Xie contributed equally to this paper.

Correspondence to Shao-Cong Sun: ssun@mdanderson.org

Abbreviations used: CNS, central nervous system; DKO, DC-conditional TBK1 KO; EAE, experimental autoimmune encephalomyelitis; IFNAR, type I IFN receptor; IKK, IκB kinase; IP, immunoprecipitation; MOG, myelin oligodendrite glycoprotein; PD1, programmed death 1; PRR, pattern-recognition receptor; qRT-PCR, quantitative RT-PCR; TBK1, TANK-binding kinase 1.

The Rockefeller University Press $30.00
J. Exp. Med. 2017 Vol. 214 No. 5 1493–1507
https://doi.org/10.1084/jem.20161524

types and stimuli used (Perry et al., 2004). However, despite the extensive in vitro studies, the in vivo physiological function of TBK1 in innate immune cells, particularly DCs, has not been investigated largely because of the embryonic lethality of the conventional *Tbk1* KO mice (Bonnard et al., 2000). Recent studies demonstrate that TBK1 can be activated by a large variety of stimulators, including PRR ligands, inflammatory cytokines, and the TNF superfamily of co-stimulatory factors (Clark et al., 2009; Jin et al., 2012; Liu et al., 2015; Yu et al., 2015). Interestingly, TBK1 activation is insufficient for triggering IRF3 activation, and not all of the TBK1 inducers are able to induce type I IFN expression (Clark et al., 2009), suggesting additional functions of TBK1.

To study the function of TBK1 in DCs, we generated DC-conditional *Tbk1* KO (hereafter called DKO) mice in the present study. We demonstrated that DC-specific deletion of *Tbk1* causes aberrant activation of T cells coupled with autoimmune symptoms, including splenomegly and lymphadenopathy as well as tissue infiltration with lymphocytes. The *Tbk1*-DKO mice also mounted stronger immune responses against tumor challenge. We provide evidence that TBK1 has a role in regulating type I IFN receptor (IFNAR) signaling. These findings suggest that TBK1 is important for DC functions in the maintenance of T cell homeostasis and prevention of autoimmune responses. Our data also suggest that targeting TBK1 in DCs may be an approach to stimulate antitumor immunity.

RESULTS

TBK1 is dispensable for DC development

To assess the function of TBK1 in DCs, we analyzed the activation of TBK1 in DCs. Phospho-immunoblotting analyses revealed that although BMDCs lacked detectable TBK1 activation unless stimulated with the TLR4 ligand LPS, splenic DCs displayed a basal level of TBK1 activation that became even more prominent in older mice, suggesting in vivo activation of TBK1 under homeostatic conditions (Fig. 1 A). To directly examine the functions of TBK1 in DCs, we generated *Tbk1*-DKO mice by crossing the *Tbk1*-flox mice (Jin et al., 2012) with CD11c-Cre mice (Fig. 1 B). The *Tbk1*-DKO and WT control mice had similar frequencies of DCs, macrophages, and neutrophils in the bone marrow and spleen, suggesting a dispensable role for DC-specific TBK1 in the development of these myeloid cells (Fig. 1 C). The frequency of conventional DCs, plasmacytoid DCs, CD8α^+ DCs, and the resident and migratory DCs in the cutaneous lymph nodes was also comparable between the WT and *Tbk1*-DKO mice (Fig. 1, D–G). These data suggested a dispensable role for TBK1 in regulating DC development.

TBK1 ablation in DCs perturbs T cell homeostasis and causes spontaneous autoimmunity

DCs play a crucial role in regulating T cell homeostasis, tolerance, and activation. Thus, we analyzed the effect of DC-specific deletion of *Tbk1* on T cell homeostasis and activation. The TBK1 deficiency did not influence T cell development in the thymus, as the *Tbk1*-DKO and WT control mice had a similar frequency of double-negative and double-positive as well as $CD4^+$ and $CD8^+$ single-positive thymocyte populations (Fig. 2 A). At a young age (10 wk), the *Tbk1*-DKO and WT control mice also had a similar frequency of total $CD4^+$ and $CD8^+$ T cells in the spleen (not depicted); however, the *Tbk1*-DKO mice had an increased frequency of activated or memory-like $CD4^+$ and $CD8^+$ T cells displaying $CD44^{hi}CD62L^{lo}$ or $CD44^{hi}$ surface markers (Fig. 2 B). This phenotype became more profound in older *Tbk1*-DKO mice (8 mo old; Fig. 2 C), coupled with strikingly elevated IFNγ-producing $CD4^+$ and $CD8^+$ effector T cells in the spleen (Fig. 2 D), although the control and *Tbk1*-DKO mice had a similar frequency of $Foxp3^+$ T reg cells in the thymus, spleen, and lymph nodes (Fig. 2 E). Consistent with their perturbed T cell homeostasis, the older *Tbk1*-DKO mice displayed autoimmune symptoms characterized by enlargement of spleen and lymph nodes, increased cellularity in these lymphoid organs, and infiltration of lymphocytes to the liver and lung (Fig. 2, F–H). Collectively, these results demonstrated an important role for DC-specific TBK1 in maintaining T cell homeostasis and preventing autoimmune responses at steady state.

TBK1 deficiency in DCs sensitizes mice to experimental autoimmunity

To further investigate the role of TBK1 in regulating immune responses, we examined the effect of DC-specific TBK1 deletion on tissue-specific autoimmunity using experimental autoimmune encephalomyelitis (EAE), an animal model of the autoimmune neuroinflammatory disease multiple sclerosis (Simmons et al., 2013). The pathogenesis of EAE involves priming of autoimmune T helper type 1 inflammatory T cells (Th1 cells) and Th17 inflammatory T cells in the periphery and their subsequent migration into the central nervous system (CNS). As expected, immunization of WT young adult (8 wk old) mice with a CNS-specific autoantigen, myelin oligodendrite glycoprotein (MOG) peptide, induced EAE disease (Fig. 3 A) and CNS infiltration of the IFN-γ–producing Th1 cell and IL-17–producing Th17 cells (Fig. 3, B–E). Importantly, the age-matched *Tbk1*-DKO mice were more sensitive to EAE induction, exhibiting earlier onset and increased severity of EAE disease (Fig. 3 A). This clinical phenotype was associated with a higher level of CNS infiltration with both total $CD4^+$ and $CD8^+$ T cells (Fig. 3, B and C) and Th1 and Th17 inflammatory effector cells (Fig. 3, D and E) in *Tbk1*-DKO mice. In addition, the spleen of the EAE-challenged *Tbk1*-DKO mice had a higher frequency and number of activated T cells, displaying the $CD62L^{lo}CD44^{hi}$ and $CD69^+$ surface markers, than that of the WT control mice (Fig. 3, F and G), whereas the frequency of T reg cells was similar between the two genotypes (Fig. 3 H). The draining lymph nodes of the *Tbk1*-DKO mice also contained a higher frequency and number of Th1 and Th17 inflammatory effector cells (Fig. 3, I and J) and antigen-specific T cells respond-

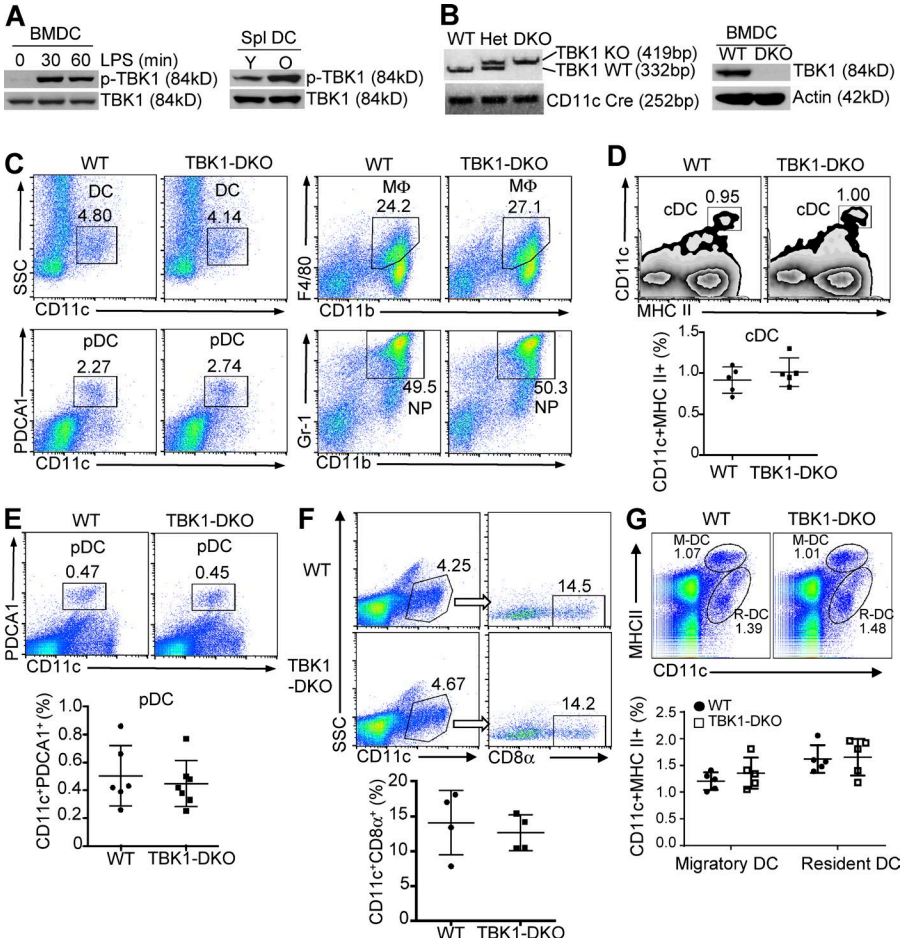

Figure 1. **DC-specific TBK1 ablation has no effect on DC development.** (A) Immunoblot analysis of phosphorylated TBK1 (p-TBK1) and total TBK1 in whole-cell lysates of BMDCs stimulated with 100 ng/ml LPS (left) and splenic DCs (Spl DC) from young (Y; 6 wk old) or old (O; 16 wk old) WT mice (right). (B) PCR analysis of TBK1 and CD11c-Cre to identify the genotype of WT, heterozygous (Het), and homozygous DC-conditional *Tbk1* KO (DKO) mice (left) and immunoblot analysis of TBK1 protein expression in BMDCs from WT and *Tbk1*-DKO mice (right). (C) Flow cytometric analysis of the frequency (numbers in quadrants) of total DCs ($CD11c^+$), plasmacytoid DCs (pDC; $CD11c^+PDCA1^+$), macrophages (MΦ; $F4/80^+CD11b^+$), and neutrophils (NP; $Gr\text{-}1^+CD11b^+$) in the bone marrow of WT and *Tbk1*-DKO mice. SSC, side scatter. (D–G) Flow cytometric analysis of the frequency of conventional DC (cDC; $CD11c^+MHCII^+$; D), plasmacytoid DC ($CD11c^+PDCA1^+$; E), $CD8\alpha^+$ DC ($CD11c^+CD8\alpha^+$; F), and migratory (M-DC; $MHCII^{hi}CD11c^+$) and resident (R-DC; $MHCII^{int}CD11c^+$) DC (G) populations in the spleen (D–F) or cutaneous LNs (G) of WT and *Tbk1*-DKO mice, presented as representative plots (top) and summary graphs (bottom). Data are representative of at least three independent experiments.

ing to MOG peptide stimulation in vitro (Fig. 3 K). Thus, DC-specific TBK1 negatively regulates induction of EAE by the CNS-specific autoantigen MOG.

TBK1 regulates antitumor immunity

A hallmark of cancer is the induction of immune tolerance (Maueröder et al., 2014). Although immune tolerance prevents the development of autoimmunity, it is a major mechanism by which cancer escapes from immune destruction (Maueröder et al., 2014). In fact, the same immune mechanisms that mediate autoimmunity also contribute to the destruction of tumors, with tumor immunotherapy often being viewed as intentional induction of autoimmune responses (Maueröder et al., 2014; Toomer and Chen, 2014). Activation of PRRs, particularly stimulator of IFN genes (STING), in DCs has been exploited as an approach to improve the efficiency of cancer immunotherapy (Seya et al., 2010; Woo et al., 2014). Although TBK1 is one of the major downstream targets of STING and many other PRRs, the DC-specific role of TBK1 in regulating antitumor immunity has remained unclear. Our finding that TBK1 had a central role in mediating the tolerant function of DCs in the context of autoimmunity and immune homeostasis raised the intriguing question of whether TBK1 promotes or suppresses the immunostimulatory function of DCs in antitumor immunity. We used an animal model of tumor immunity that involves challenge of mice with mouse B16 melanoma cells. The *Tbk1*-DKO mice displayed a significantly stronger ability to suppress tumor growth, coupled with increased survival rate upon tumor challenge, compared with the WT control mice (Fig. 4, A and B). Consistently, the *Tbk1*-DKO mice had increased frequency of tumor-infiltrating $CD4^+$ and $CD8^+$ effector T cells producing IFN-γ (Fig. 4, C and D). The draining lymph nodes of the tumor-bearing *Tbk1*-DKO mice also contained an increased frequency and number of IFN-γ–positive $CD4^+$ and $CD8^+$ effector T cells compared with those of the WT mice (Fig. 4 E), whereas the frequency of T reg cells was not increased (Fig. 4 F). Parallel studies revealed that the *Tbk1*-DKO mice also displayed enhanced antitumor immunity in two other tumor models, induced with the EG7-OVA (Fig. 4, G and H) and EL4 (Fig. 4, I and J) thymoma cells, respectively.

Programmed death 1 (PD1) is a tolerance molecule that is expressed on effector T cells and mediates inhibition of antitumor T cell responses, and an anti-PD1 neutralizing antibody has demonstrated promise in cancer immunotherapy (Zou et al., 2016). Because TBK1 functions in DCs to regulate T cell tolerance, we tested whether TBK1 deletion

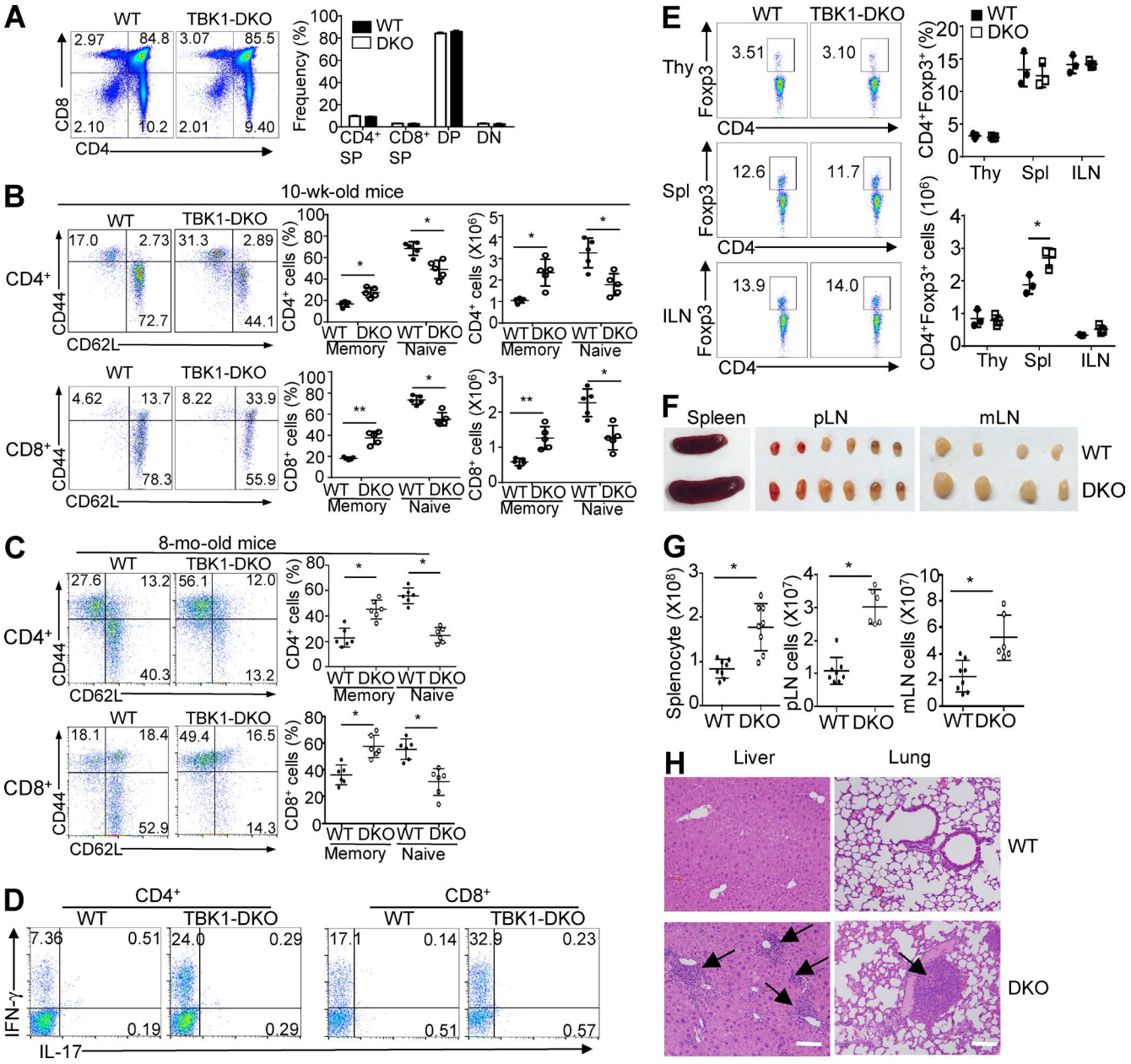

Figure 2. **TBK1 deficiency in DCs impairs T cell homeostasis and causes autoimmunity.** (A) Flow cytometric analysis of thymocytes in *Tbk1*-DKO and WT control mice, with the percentage of double-negative (DN), double-positive (DP), and $CD4^+$ and $CD8^+$ single-positive (SP) populations summarized based on three WT and three *Tbk1*-DKO mice (8 wk old). Data are presented as means ± SD. (B and C) Flow cytometric analysis of the frequency and absolute number of naive ($CD44^{lo}CD62L^{hi}$) and memory-like ($CD44^{hi}CD62L^{lo}$ for $CD4^+$ and $CD44^{hi}$ for $CD8^+$ T cells) $CD4^+$ and $CD8^+$ T cells in total splenocytes from WT and *Tbk1*-DKO mice (10 wk and 8 mo old). Data are presented as representative plots (left) and summary graphs (right). (D) Flow cytometric analysis of the percentage of IFN-γ–producing and IL-17–producing $CD4^+$ and $CD8^+$ T cells in the spleen of 8-mo-old WT and *Tbk1*-DKO mice. (E) Frequency of $CD4^+Foxp3^+$ T reg cells in the thymus (Thy), spleen (Spl), and inguinal lymph nodes (ILN) of 10-wk-old WT and *Tbk1*-DKO mice, presented as a representative FACS plot (left) and summary graph based on multiple mice (right). (F and G) Representative images (F) and total cell number (G) of spleen, peripheral lymph nodes (pLN), and mesentery lymph nodes (mLN) of WT and *Tbk1*-DKO mice (8 mo old). (H) Hematoxylin-eosin staining of the indicated tissue sections from 8-mo-old WT and *Tbk1*-DKO mice, showing immune cell infiltrations in the *Tbk1*-DKO tissues (arrows). Bars, 100 µm. Data are representative of three or more independent experiments. *, $P < 0.05$; **, $P < 0.01$.

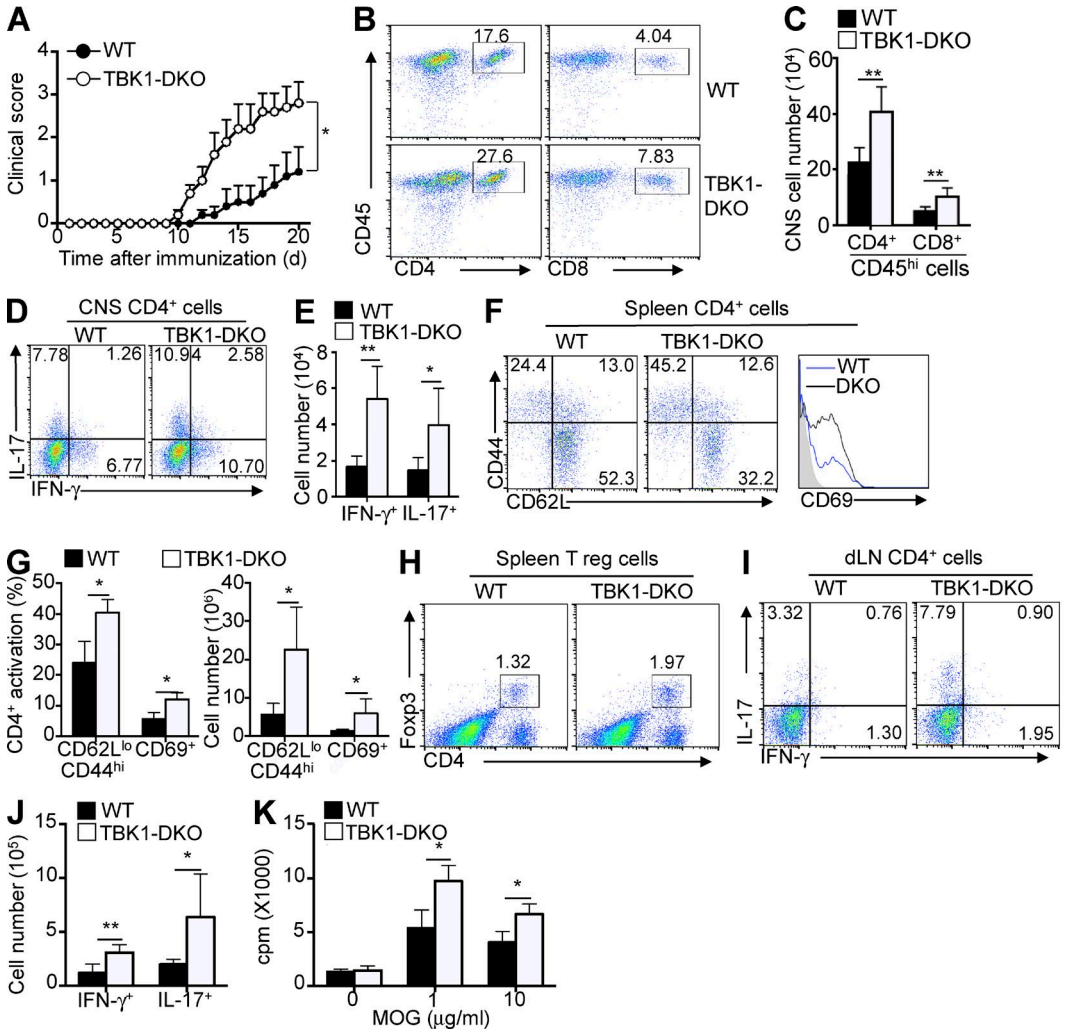

Figure 3. **DC-specific TBK1 deletion promotes T cell responses in EAE induction.** (A) Mean clinical scores of age- and sex-matched WT and *Tbk1*-DKO mice (8 wk old) subjected to MOG_{35-55}-induced EAE. n = 5/group. (B and C) Flow cytometric analysis of T cells infiltrating into the CNS (brain and spinal cord) of day-15 EAE-induced mice, presented as representative plots (B) and absolute number (C). (D and E) Frequency and absolute number of IFN-γ– and IL-17–producing effector T cells in the CNS of day-15 MOG_{35-55}-immunized WT and *Tbk1*-DKO mice, shown as a representative plot (D) and a summary graph (E). (F and G) Frequency and absolute number of $CD62L^{lo}CD44^{hi}$ and $CD69^+$ $CD4^+$ effector T cells in the spleen of day-15 MOG_{35-55}-immunized mice, presented as representative plots (F) and summary graphs (G). (H) Frequency of spleen T reg cells from day-15 EAE-induced mice. (I and J) Frequency and absolute number of IFN-γ– and IL-17–producing $CD4^+$ T cells in the draining lymph node (dLN) of day-15 EAE-induced mice. (K) Thymidine incorporation cell proliferation assays of splenic T cells from day-15 EAE-induced mice, stimulated in vitro with the indicated concentrations of MOG peptide. Data are representative of at least three independent experiments and are presented as means ± SD. *, $P < 0.05$; **, $P < 0.01$.

could synergize with the action of anti-PD1 in the induction of tumor rejection using the B16 melanoma model. In this experiment, we used B16F10 melanoma cells (lacking the surrogate antigen OVA), which are known as a low immunogenecity tumor model. Under these conditions, the DC-specific TBK1 deletion promoted tumor rejection to an extent that was similar to that caused by anti-PD1 injection (Fig. 4 K). Remarkably, the combination of anti-PD1 treatment and TBK1 deletion resulted in a strong synergistic effect leading to profoundly reduced tumor growth and increased mouse survival (Fig. 4, K and L).

DC-based cancer immunotherapy has become a promising approach of cancer treatment (Anguille et al., 2014). To further examine the DC-specific role of TBK1, we used an animal model of DC-based therapy. After inoculation of B6 mice with B16 cells expressing the surrogate antigen OVA, we injected OVA-pulsed WT or TBK1-deficient DCs into the tumor-bearing mice. Compared with the WT DCs, the TBK1-deficient DCs were significantly more potent in suppressing the tumor growth and inducing tumor-infiltrating effector T cells (Fig. 4, M and N). This phenotype was not caused by altered properties of DC homing, as transferred

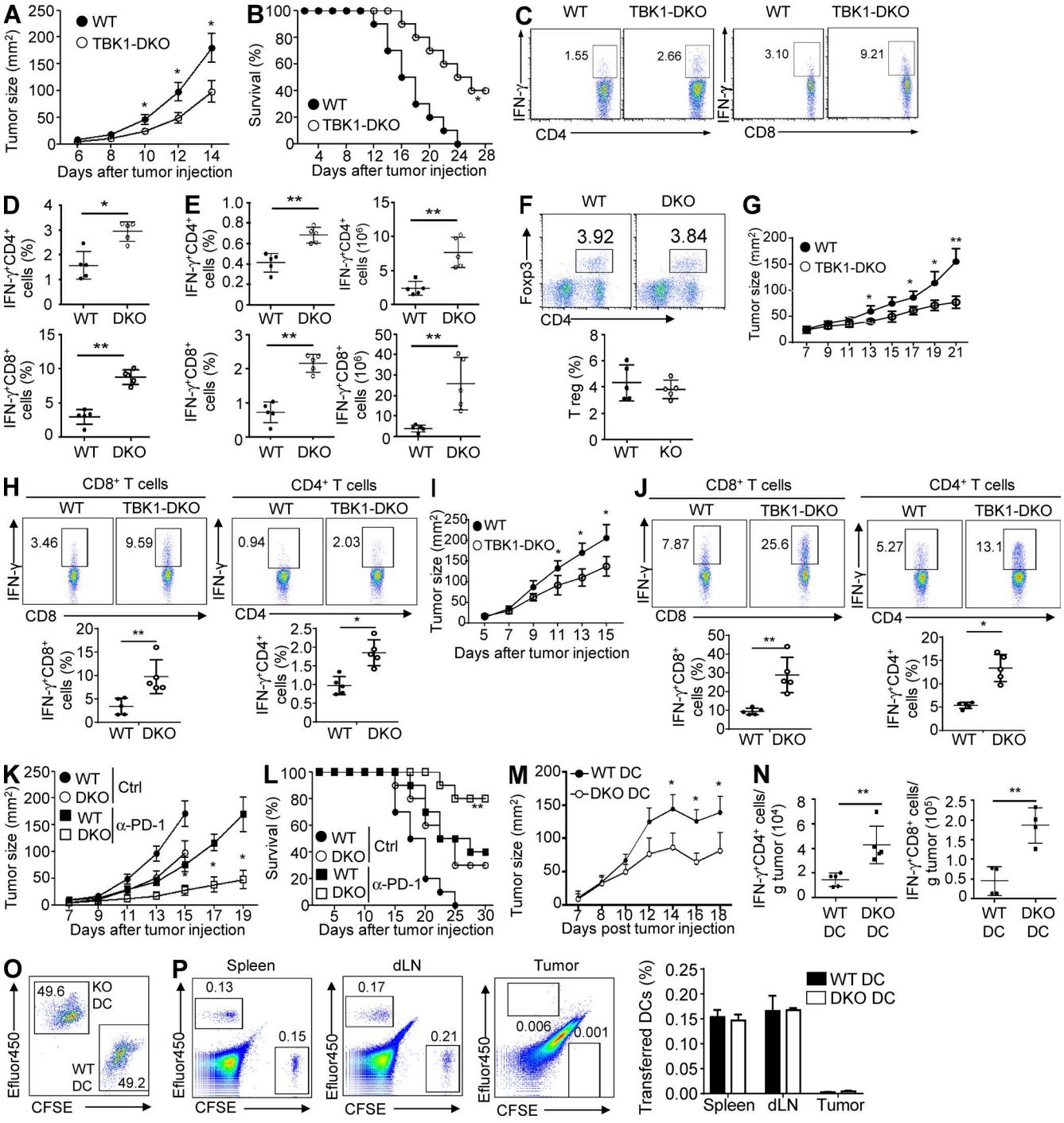

Figure 4. **TBK1 deficiency in DCs promotes antitumor immunity.** (A and B) Tumor growth (A) and survival (B) curves of WT and *Tbk1* DKO mice injected s.c. with B16-OVA melanoma cells. $n = 10$. (C and D) Flow cytometric analysis of the frequency (C) and absolute cell numbers (D) of IFN-γ–producing $CD4^+$ and $CD8^+$ T cells in tumors of WT and *Tbk1*-DKO mice injected s.c. with B16-OVA melanoma cells (day 16 after injection). (E and F) Flow cytometric analysis of the percentage and absolute cell numbers of IFN-γ–producing $CD4^+$ and $CD8^+$ T cells (E) or percentage of T reg cells (F) in draining lymph nodes of WT and *Tbk1*-DKO mice injected s.c. with B16-OVA melanoma cells (day 16 after injection). Cells were stimulated with OVA peptide for 5 h after intracellular staining. (G–J) Tumor growth (G and I) and flow cytometric analysis of IFN-γ–producing $CD4^+$ and $CD8^+$ T cells in draining lymph nodes (H and J) of WT and *Tbk1*-DKO mice injected s.c. with EG7-OVA (G and H) or EL4 (I and J) thymoma cells (day 22 for EG7-OVA and day 16 for EL4 after injection). (K and L) Tumor growth (K) and survival (L) curves of WT and *Tbk1*-DKO mice injected s.c. with B16 melanoma cells without the surrogate antigen OVA ($n = 10$) followed by i.p. injection with PD-1 antibody on days 7, 10, and 13. Ctrl, control. (M) Tumor growth curve of WT mice injected s.c. with B16-OVA melanoma cells and then treated (on day 7) i.v. with WT or *Tbk1*-DKO BMDCs that were pulsed with OVA peptide and matured with LPS. (N) Flow cytometric analysis of the ab-

WT and TBK1-deficient DCs displayed similar homing patterns (Fig. 4, O and P). Collectively, these results suggest that targeting TBK1 in DCs may be an approach to promote antitumor immunity.

TBK1 deficiency promotes the immunostimulatory functions of DCs

To understand the mechanism by which TBK1 regulates DC functions in antitumor immunity, first, we examined TBK1 activation in DCs of tumor-bearing mice based on its phosphorylation. Consistent with the phospho-immunoblot assays (Fig. 1 A), flow cytometry detected TBK1 phosphorylation in lymph node DCs of untreated mice, and the level of TBK1 phosphorylation was elevated in draining lymph node DCs of B16 tumor-bearing mice (Fig. 5 A). Interestingly, TBK1 deficiency caused an increase in the expression of the co-stimulatory molecules CD80 and CD86 in splenic DCs of untreated mice, and this phenotype was more profound in DCs isolated from tumors of B16 tumor-bearing mice (Fig. 5, B and C). This finding prompted us to examine whether the TBK1 deficiency promoted the T cell–priming function of DCs. We used an in vitro model involving activation of OTII T cells with DCs pulsed with a specific peptide, chicken OVA 323–339. For measuring cell proliferation, the OTII T cells were labeled with CFSE. Compared with WT DCs, the TBK1-deficient DCs stimulated stronger proliferation of OTII T cells, as measured based on CFSE dilution (Fig. 5 D). These results suggest that TBK1 deficiency promotes the immunostimulatory function of DCs.

TBK1 regulates a subset of IFN-responsive genes in DCs

To further elucidate the molecular mechanism by which TBK1 regulates DC function, we examined the effect of TBK1 deficiency on gene induction by the TLR4 ligand LPS. As expected, LPS-stimulated expression of *Ifna* and *Ifnb* genes was impaired in TBK1-deficient DCs (Fig. 5 E). Moreover, the TBK1 deficiency inhibited the induction of the immunosuppressive cytokine IL-10 and promoted the induction of several immunostimulatory cytokines, including IL-1β, IL-12, and IL-23 (Fig. 5 E).

Although the in vitro studies provided insight into the role of TBK1 in regulating TLR-stimulated gene expression, it was still unclear how TBK1 regulated the DC gene expression profile under homeostatic conditions in vivo. To this end, we analyzed the gene expression profile of WT and TBK1-deficient splenic DCs by RNA sequencing. This experiment, based on three independent samples, revealed significant alterations in the expression of several genes (Fig. 5, F and G), most notably the enhanced expression of a large subset of IFN-responsive genes in the TBK1-deficient DCs (Fig. 5 H). As a previous study identified a DC-specific role for the NF-κB–activating kinase IKKβ in regulating immune homeostasis and tolerance (Baratin et al., 2015), we examined the possible connection of TBK1 with the NF-κB pathway. We analyzed the RNA sequencing data for NF-κB gene signature and included the IFN-responsive gene *Ifi202b* as a control. Unlike *Ifi202b*, the NF-κB signature genes were not substantially affected by the TBK1 deficiency (Fig. 5 I). The TBK1 deficiency also did not inhibit TLR-stimulated activation of NF-κB or mitogen-activated protein kinases (not depicted). To further confirm the role of TBK1 in regulating IFN-responsive gene expression, we performed quantitative RT-PCR (qRT-PCR) assays using freshly isolated WT and TBK1-deficient spleen DCs. Several, although not all, of the IFN-responsive genes tested were found to be up-regulated in the TBK1-deficient DCs (Fig. 5 J). We found that the TBK1 deficiency did not significantly affect the homeostatic expression level of *Ifna* and *Ifnb* genes (Fig. 5 J), suggesting a novel function of TBK1 in regulating IFN receptor signaling. Indeed, upon in vitro starvation and restimulation with IFN-β, the TBK1-deficient DCs also expressed profoundly higher levels of IFN-responsive genes than the WT control DCs (Fig. 5 K). These results are intriguing as type I IFN signaling is known to promote antitumor immunity and mediate systemic autoimmunity (Hall and Rosen, 2010; Fuertes et al., 2013).

Deletion of IFNAR1 prevents aberrant T cell activation and autoimmunity in TBK1 DKO mice

To examine whether TBK1 functions in conjunction with type I IFN signaling in the regulation of immune tolerance, we crossed the *Tbk1*-DKO mice with *Ifnar1*-KO mice. As expected, DC-specific deletion of TBK1 in IFNAR-WT genetic background caused a drastic increase in the frequency of $CD44^{hi}CD62L^{lo}$ effector/memory-like $CD4^+$ T cells producing the effector cytokine IFN-γ (Fig. 6, A and B). Deletion of IFNAR1 did not substantially alter the frequency of effector/memory-like $CD4^+$ T cells or IFN-γ–producing $CD4^+$ T cells. However, the IFNAR1 ablation largely corrected the aberrant T cell activation phenotype of the *Tbk1*-DKO mice (Fig. 6, A and B). The IFNAR1 deficiency also suppressed the autoimmune symptoms of the *Tbk1*-DKO mice, including splenomegly and lymphadenopathy (Fig. 6 C) and immune cell infiltration into the liver and lung (Fig. 6 D).

We also examined the role of IFN signaling in the antitumor immunity of TBK1-deficient DCs by performing DC-based tumor immunotherapy. Under these conditions, the IFNAR1 deficiency only moderately reduced the tumor-

solute cell numbers of IFN-γ–producing $CD4^+$ and $CD8^+$ T cells in tumors of the mice from M (day 18 after injection). (O and P) CFSE-labeled WT BMDCs and efluor450-labeled *Tbk1*-DKO BMDCs were subjected to flow cytometry analysis (O) or injected into day-7 B16 tumor-bearing WT mice for 18 h followed by flow cytometric detection of the transferred DCs in spleen, draining LNs (dLN), or tumor (P). Data are representative of at least three independent experiments and are presented as means ± SD. *, $P < 0.05$; **, $P < 0.01$.

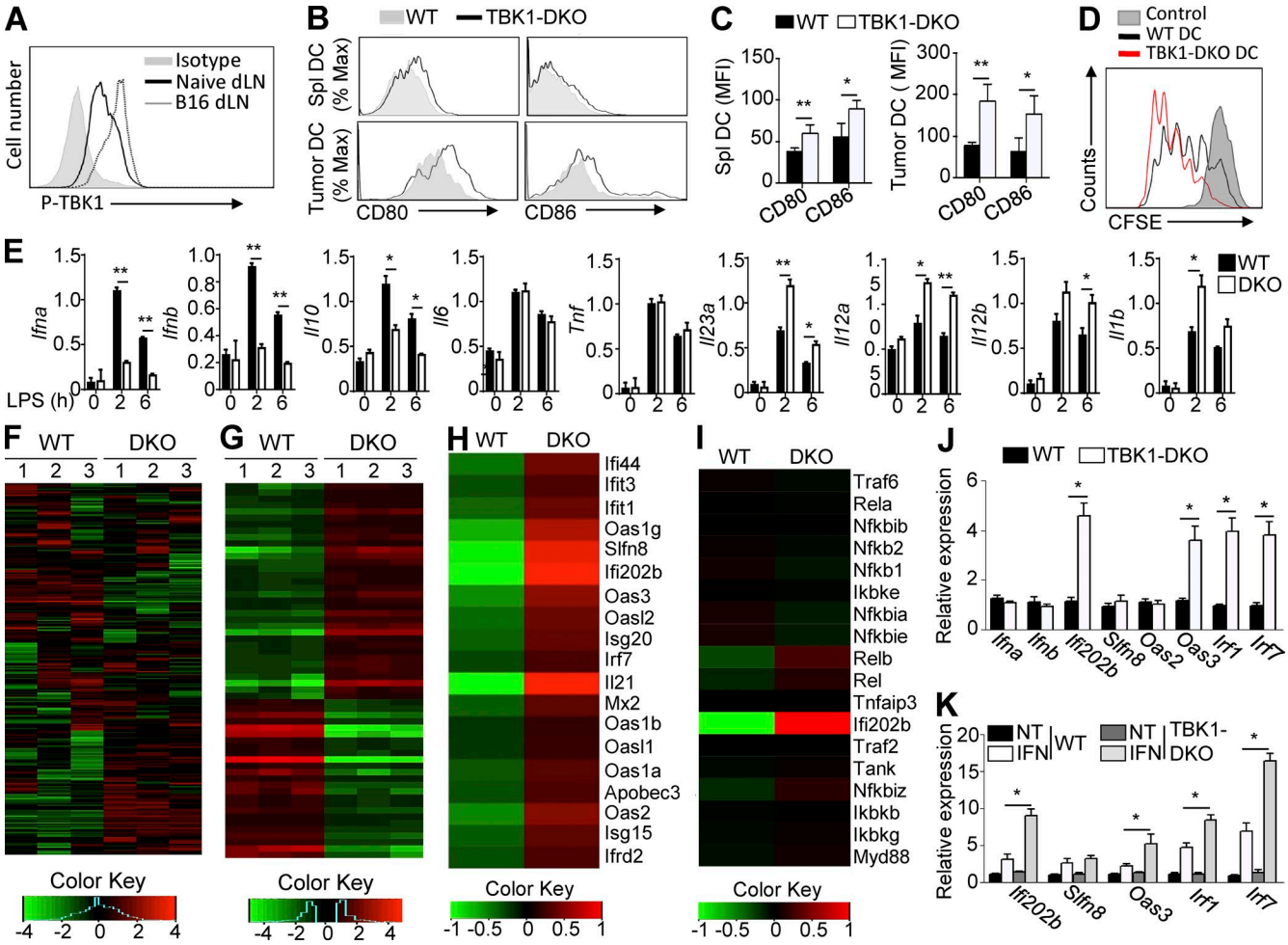

Figure 5. **TBK1 regulates the expression of IFN-response genes in DCs.** (A) Flow cytometric analysis of phosphorylated TBK1 (P-TBK1) in CD11c$^+$ DCs isolated from the draining LNs (dLN) of untreated (naive) mice or mice injected s.c. with B16 melanoma cells. (B and C) Flow cytometric analysis of CD80 and CD86 expression on WT or *Tbk1*-DKO spleen CD11c$^+$ DCs (Spl DC) and B16 tumor-infiltrating CD11c$^+$ DCs (Tumor DC). MFI, mean fluorescence intensity. (D) Flow cytometric analysis to measure the proliferation of CFSE-labeled OTII T cells incubated with either medium control or OVA-pulsed WT and *Tbk1*-DKO spleen DCs. (E) qRT-PCR analysis of the indicated genes using LPS-stimulated splenic DCs derived from WT and *Tbk1*-DKO mice (8 wk old). (F–I) RNA-sequencing analysis using splenic DCs freshly isolated from 8-wk-old WT and *Tbk1*-DKO mice (each group has three samples), showing a heat map of highly variable genes (top 1,500; F), genes with adjusted p-value <0.01 and log2 fold-change >1.5 (G), IFN-responsive genes (H), and NF-κB signature genes using the IFN-responsive gene Ifi202b as a positive control (I). (J) qRT-PCR analysis of the indicated genes in freshly isolated splenic DCs from WT and *Tbk1*-DKO mice (8 wk old). (K) qRT-PCR analysis of the indicated genes using splenic DCs from J that were starved for 6 h and then either not treated (NT) or stimulated with IFN-β for 3 h. Data are representative of three independent experiments and are presented as means ± SD. *, P < 0.05; **, P < 0.01.

suppression function of the DCs, whereas TBK1 deficiency greatly enhanced the tumor-suppression function of the DCs (Fig. 6 E). Moreover, in the *Ifnar1*-null background, the *Tbk1*-DKO and WT mice no longer had differences in mediating tumor rejection (Fig. 6 E). Collectively, these results suggest that the DC-specific functions of TBK1 involve modulation of IFNAR1 signaling.

TBK1 mediates STAT3 serine phosphorylation

A major signaling event induced by type I IFNs is activation of STAT1 via its phosphorylation at tyrosine 701 (Y701) and serine 727 (S727; Ivashkiv and Donlin, 2014). Under homeostatic conditions, STAT1 was constitutively, although moderately, phosphorylated at Y701, which appeared to be dependent on type I IFNs, as the STAT1 Y701 phosphorylation was abolished in IFNAR1-deficient DCs (Fig. 7 A, left). Moreover, TBK1 deficiency caused an increase in STAT1 Y701 phosphorylation, but it did not affect the S727 phosphorylation of STAT1 (Fig. 7 B, left). Because TBK1 is a serine/threonine kinase, the enhanced STAT1 Y701 phosphorylation was obviously caused by indirect effect. In this regard, STAT3 is known to be activated by type I IFNs and inflammatory cytokines and be involved in negative regulation of STAT1 activation and type I IFN responses (Wang et al., 2011; Ivashkiv and Donlin, 2014).

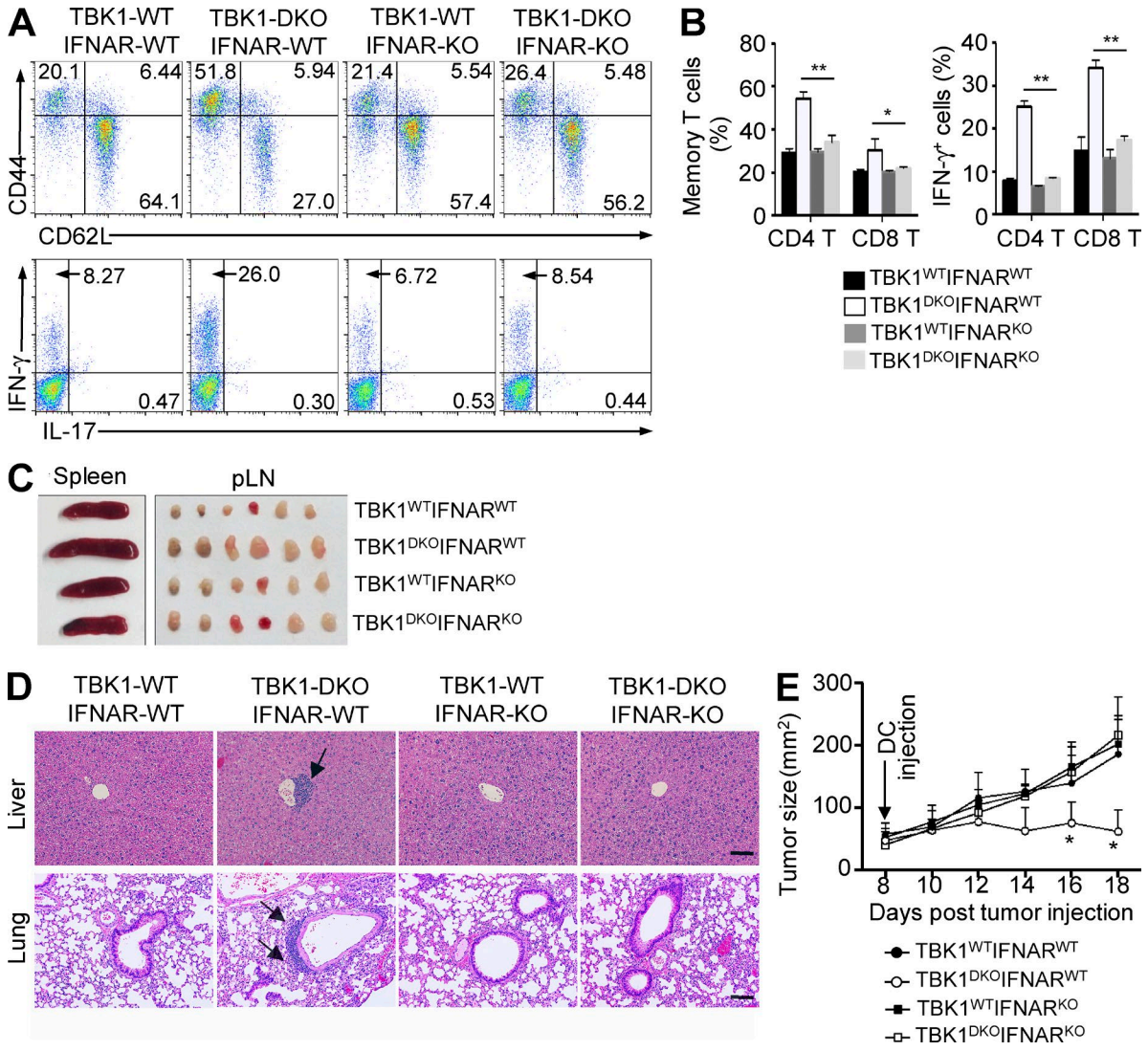

Figure 6. **Deletion of IFNAR1 prevents autoimmunity and suppresses antitumor immunity in *Tbk1* DKO mice.** (A) Frequency of naive ($CD44^{lo}CD62L^{hi}$) and memory ($CD44^{hi}CD62L^{lo}$) $CD4^+$ T cells and IFN-γ–producing $CD4^+$ T cells in the spleen of age- and sex-matched mice with the indicated genotype (4 mo old). (B) Summary data of flow cytometric analysis of memory $CD4^+$ ($CD4^+CD44^{hi}CD62^{lo}$) and $CD8^+$ ($CD8^+CD44^{hi}$) T cells in the spleen described in A. (C) Representative spleen and peripheral lymph node (pLN) images of age- and sex-matched mice with the indicated genotype (4 mo old). (D) Hematoxylin-eosin staining of the indicated tissue sections from age- and sex-matched mice (5 mo old), showing immune cell infiltrations in the *Tbk1*-DKO tissues (arrows). Bars, 100 µm. (E) Growth curve of tumors ($n = 5$) of WT mice that were injected s.c. with B16-OVA melanoma cells and then treated i.v. by BMDCs with the indicated genotype that were pulsed with OVA peptide and matured with LPS. Data are representative of at least three independent experiments and are presented as means ± SD. *, $P < 0.05$; **, $P < 0.01$.

Furthermore, STAT3 is crucial for the tolerant function of DCs, and DC-conditional deletion of STAT3 in mice results in T cell activation and autoimmunity (Cheng et al., 2003). Thus, we examined STAT3 activation based on its phosphorylation at Y705 and S727. Interestingly, DCs displayed a high level of S727 phosphorylation, although only moderate Y705 phosphorylation, and of STAT3, and the STAT3 S727 phosphorylation was partially inhibited in IFNAR1-deficient DCs (Fig. 7 A, right). Moreover, the TBK1 deficiency severely attenuated the S727 phosphorylation of STAT3 in DCs (Fig. 7 B, right). This intriguing result prompted us to determine the role of DC-specific STAT3 in regulating IFN-responsive genes and immune tolerance using DC-conditional *Stat3* KO (*Stat3*-DKO) mice. Similar to the TBK1-deficient DCs, the STAT3-deficient DCs had up-regulated expression of several IFN-responsive genes (Fig. 7 C). Furthermore, as seen with the *Tbk1*-DKO mice, the *Stat3*-DKO mice had increased frequency of $CD4^+$ and $CD8^+$ T cells with activated phenotype (Fig. 7 D).

A recent study has identified a conserved sequence motif at the phosphorylation site of several TBK1 substrate

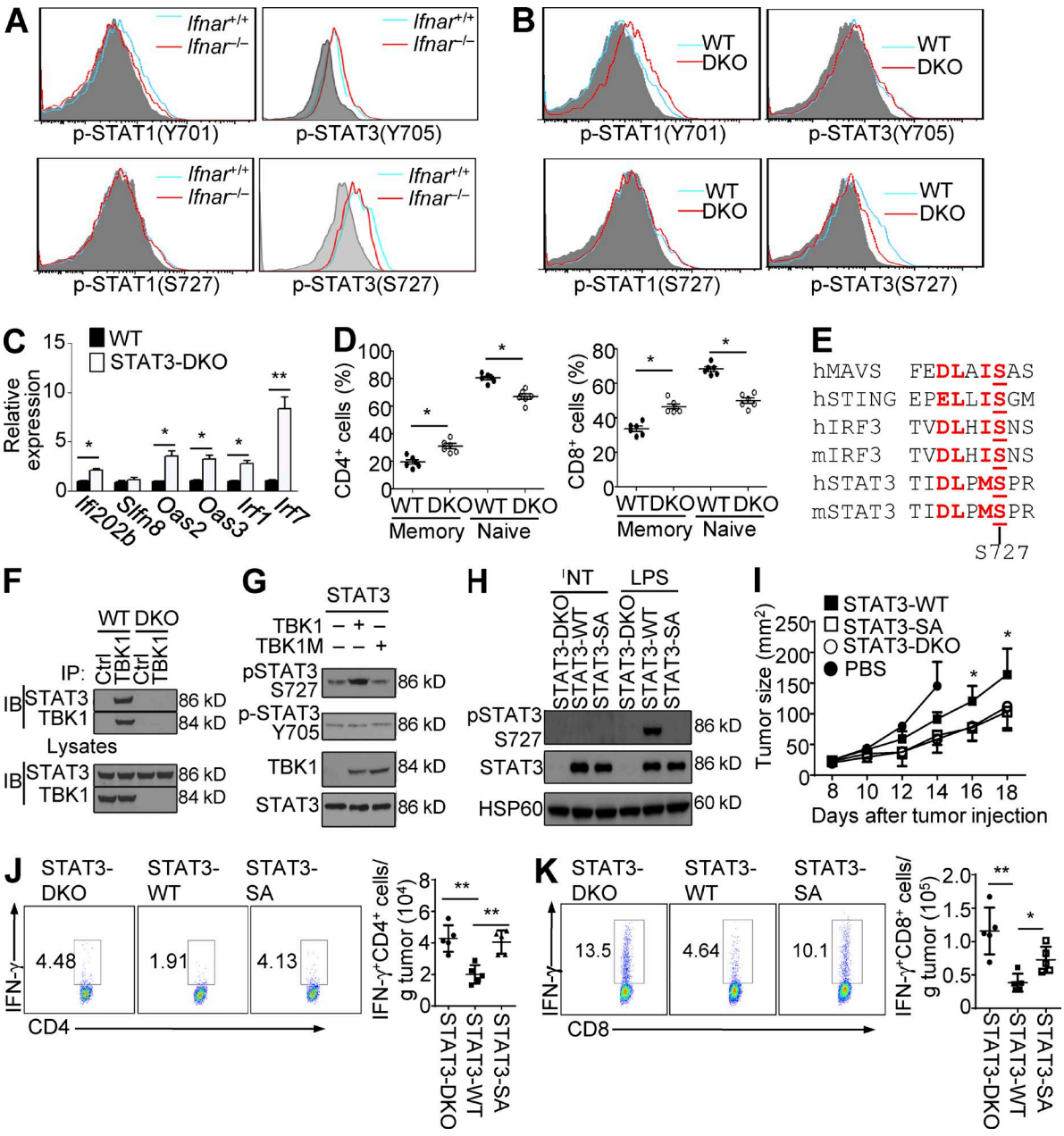

Figure 7. **TBK1 mediates STAT3 phosphorylation in DCs.** (A and B) Flow cytometric analysis of tyrosine (Y701) and serine (S727) phosphorylation of STAT1 and STAT3 in freshly isolated splenic CD11c$^+$ DCs from 8-wk-old *Ifnar*$^{+/+}$ and *Ifnar*$^{-/-}$ mice (A) or 8-wk-old WT and *Tbk1*-DKO mice (B). (C) qRT-PCR analysis of the indicated genes in freshly isolated splenic CD11c$^+$ DCs from age- and sex-matched WT and *Stat3*-DKO mice (8 wk old). (D) Flow cytometric analysis of naive (CD44^{lo}CD62L^{hi}) and memory-like (CD44^{hi}CD62L^{lo}) CD4$^+$ and CD8$^+$ T cells in splenocytes from age- and sex-matched WT and *Stat3*-DKO mice (3 mo old). (E) Sequence alignment of the S727 phosphorylation site of STAT3 with the phosphorylation site of several known TBK1 substrate proteins. Conserved residues are shown in red, and the phosphorylation serine is underlined. MAVS, mitochondrial antiviral-signaling protein. (F) Lysates of WT or *Tbk1*-DKO splenic DCs were subjected to IP using anti-TBK1 or a control Ig (Ctrl); TBK1 and TBK1-associated STAT3 were detected by immunoblotting (IB). (G) Immunoblot analysis of STAT3 phosphorylation in HEK293T cells transfected with STAT3 along with either TBK1 or a catalytically inactive TBK1 mutant (TBK1M). (H) Immunoblot analysis of S727 phosphorylated STAT3, total STAT3, and loading control HSP60 in BMDCs prepared from STAT3-WT, *Stat3*-DKO, or STAT3-S727A mutant (STAT3-SA) mice, either not treated (NT) or stimulated with LPS. (I) Tumor growth curve of WT mice injected s.c. with B16-OVA melanoma cells and then injected i.v. (on day 7) with BMDCs described in H that were pulsed with OVA peptide and matured with LPS. (J and K) Tumor-infiltrating CD4$^+$ (J) and CD8$^+$ (K) T cells from the tumor-bearing mice described in I, presented as representative FACS plots (left) and summary graphs based on multiple mice (right). Data are representative of three or more independent experiments and are presented as means ± SD. *, $P < 0.05$; **, $P < 0.01$.

proteins (Liu et al., 2015). Interestingly, the serine phosphorylation site (S727) of STAT3 also has such a conserved sequence motif (Fig. 7 E). TBK1 physically interacted with STAT3, as shown by a coimmunoprecipitation (co-IP) assay (Fig. 7 F). Furthermore, TBK1, but not a catalytically inactive TBK1 mutant, potently phosphorylated S727 of STAT3 (Fig. 7 G). Using a DC-based tumor therapy model, we found that DCs deficient in STAT3 or expressing S727A mutant of STAT3 displayed significantly higher tumor-suppressing activity (Fig. 7, H and I). The STAT3-KO and STAT3-SA DCs also induced a significantly higher level of tumor-infiltrating $CD4^+$ and $CD8^+$ T cells producing IFN-γ compared with the WT DCs (Fig. 7, J and K). These results indicated that the role of TBK1 in regulating DC functions involves phosphorylation of STAT3, although the possibility for TBK1 to target additional signaling factors in DCs cannot be excluded.

DISCUSSION

TBK1 and IKKε are known as kinases that mediate induction of type I IFNs in response to various PRR signals (Hiscott, 2007). In addition to the PRR ligands, many other agents, such as inflammatory cytokines, the TNF superfamily of co-stimulatory factors, and T cell receptor stimuli, stimulate TBK1 activation, although not all of these agents induce type I IFN expression (Clark et al., 2009; Jin et al., 2012; Liu et al., 2015; Yu et al., 2015). Emerging evidence suggests that TBK1 has additional roles in the regulation of immune system functions (Jin et al., 2012; Yu et al., 2015). Our present study demonstrated a DC-specific function of TBK1 in the regulation of immune homeostasis and tolerance. DC-specific deletion of TBK1 caused aberrant activation of T cells, a phenotype that became particularly striking in older mice. Consistently, the older *Tbk1*-DKO mice displayed overt autoimmune symptoms, and the young *Tbk1*-DKO mice were also more sensitive to the induction of a T cell–dependent experimental autoimmune disease, EAE.

A major phenotype of the *Tbk1*-DKO mice was the perturbation of T cell homeostasis and spontaneous development of autoimmunity at older ages. The TBK1 deficiency in DCs did not alter the frequency of T reg cells in the thymus, spleen, and lymph nodes. Although it remains to be examined whether T reg function is impaired in the *Tbk1*-DKO mice, DCs are known to mediate immune tolerance by both promoting T reg cell induction and inducing T cell anergy (Mahnke et al., 2002). It is thought that DCs with immature or semi-mature phenotypes, characterized by low surface expression of co-stimulatory molecules and MHC class II, are important for maintaining immune tolerance (Mahnke et al., 2002; Dalod et al., 2014). We found that TBK1-deficient DCs had elevated levels of CD80 and CD86 under both homeostatic and tumor-challenged conditions and displayed stronger ability to prime T cells in vitro. The perturbed immune homeostasis may also contribute to the enhanced sensitivity of the *Tbk1*-DKO mice to the inducible autoimmunity EAE. Similarly, because interruption of immune tolerance promotes antitumor immunity, the perturbed immune homeostasis and tolerance also likely contributed the enhanced antitumor immunity in the *Tbk1*-DKO mice.

A recent study suggests that the IKK/NF-κB signaling pathway functions in DCs to regulate immune tolerance (Baratin et al., 2015). By performing RNA sequencing, we demonstrated that TBK1 deficiency in DCs had no obvious effect on the expression of NF-κB signature, which was consistent with the involvement of TBK1 in IRF3 but not NF-κB signaling pathways. Under homeostatic conditions, the TBK1 deletion in DCs also did not influence the expression of type I IFNs. Interestingly, the TBK1-deficient DCs displayed a gene expression signature characterized by up-regulated expression of a subset of IFN-responsive genes. The TBK1-deficient DCs also had several down-regulated genes, most notably Adamdec1 (unpublished data), which encodes metzincin metalloprotease known to be involved in regulation of intestinal immunity and inflammation (O'Shea et al., 2016). The role of Adamdec1 in DC function remains to be further studied. Nevertheless, the RNA-sequencing results uncovered an intriguing function of TBK1 in regulating IFN AR1 signaling. When stimulated in vitro, the TBK1-deficient DCs were also hyper-responsive to IFN-β–induced gene expression, further emphasizing a negative function of TBK1 in regulating IFNAR signaling. Moreover, deletion of IFN AR1 largely corrected the abnormalities of the *Tbk1*-DKO mice in T cell homeostasis and inhibited the development of spontaneous autoimmunity. These results suggest TBK1-mediated negative regulation of IFNAR signaling contributes to the maintenance of T cell homeostasis and immune tolerance.

A major signaling event resulting from the binding of type I IFNs to IFNAR is activation of the transcription factor STAT1. In splenic DCs, STAT1 is constitutively phosphorylated at Y701 in an IFNAR-dependent manner. Consistent with the up-regulated expression of IFN-responsive genes, the TBK1-deficient DCs had enhanced phosphorylation of STAT1 at Y701. However, because TBK1 has no tyrosine kinase activity, this result was obviously caused by an indirect effect of the TBK1 deficiency. In this regard, STAT3 has been shown to negatively regulate IFN responses and attenuate the induction of a subset of STAT1-target genes (Ho and Ivashkiv, 2010; Wang et al., 2011). STAT3 deletion in DCs breaks immune tolerance and causes T cell activation in mice (Cheng et al., 2003; Melillo et al., 2010; Li et al., 2016). STAT3 is activated by inflammatory cytokines and type I IFNs via phosphorylation at both Y705 and S727 (Ng and Cantrell, 1997; Shen et al., 2004). Our data suggest that TBK1 may function as a kinase mediating S727 phosphorylation of STAT3. Loss of TBK1 in DCs reduced STAT3 S727 phosphorylation, and overexpressed TBK1 could phosphorylate STAT3 S727. Interestingly, S727 of STAT3 is located in a sequence motif that shares homology with the typical TBK1 phosphorylation sites in other proteins.

In conclusion, we demonstrated a DC-specific role for TBK1 in regulating T cell homeostasis and autoimmune

responses. Our data also suggest that targeting TBK1 in DCs promotes antitumor immunity, implicating TBK1 as a potential therapeutic target in DC-based cancer immunotherapy. These findings provide additional evidence that TBK1 is a kinase with diverse immunoregulatory functions in addition to mediating antiviral innate immunity.

MATERIALS AND METHODS

Mice

Tbk1-floxed mice (in C57BL/6-129S background) were generated using a LoxP targeting system (Taconic; Jin et al., 2012). The *Tbk1*-floxed mice were crossed with CD11c-Cre transgenic mice (The Jackson Laboratory) in B6 background to produce age-matched $Tbk1^{+/+}CD11c^{Cre}$ (termed WT) and $Tbk1^{fl/fl}CD11c^{Cre}$ (termed *Tbk1*-DKO) mice for experiments. In some experiments, these mice were further crossed with the $Ifnar^{-/-}$ mice to generate $Tbk1^{WT}Ifnar^{KO}$ and $Tbk1^{DKO}Ifnar^{KO}$ mice, respectively. $Stat3^{fl/fl}$ mice, provided by S. Akira (Osaka University, Osaka, Japan; Takeda et al., 1998), were crossed with CD11c-Cre transgenic mice to produce age-matched $Stat3^{+/+}CD11c^{Cre}$ (termed WT) and $Stat3^{fl/fl}$-$CD11c^{Cre}$ (termed *Stat3*-DKO) mice for experiments. Mice carrying STAT3 S727A mutation (called STAT3-SA mice) were as previously described (Shen et al., 2004). Mice were maintained in a specific pathogen–free facility, and all animal experiments were in accordance with protocols approved by the Institutional Animal Care and Use Committee of the University of Texas MD Anderson Cancer Center.

Plasmids, antibodies, and reagents

FLAG-tagged STAT3 (STAT3-Flag pRc/CMV) was obtained from Addgene. FLAG-TBK1 and its catalytically inactive mutant (K38A) were provided by C. Wang (Shanghai Institutes for Biological Sciences, Shanghai, China). Antibodies for TBK1, STAT3, phosho-STAT3 (Ser727), and phospho-STAT1 (Tyr701) were purchased from Cell Signaling Technology. Antibodies used for flow cytometry were from eBioscience. Anti–m–PD-1 (clone J43) and isotype control IgG (hamster IgG) antibodies were from Bio X Cell. LPS (derived from *Escherichia coli* strain 0127:B8) was from GE Healthcare, and recombinant mouse IFN-β was from R&D Systems.

Histology

Organs were removed from WT or *Tbk1*-DKO mice, fixed in 10% neutral buffered formalin, embedded in paraffin, and sectioned for staining with hematoxylin and eosin.

Induction and assessment of EAE

For active EAE induction, age- and sex-matched mice (8–10 wk) were immunized s.c. with 300 µg $MOG_{35–55}$ peptide mixed in CFA (Sigma-Aldrich) containing 5 mg/ml heat-killed *Mycobacterium tuberculosis* H37Ra (Difco). 200 ng pertussis toxin (List Biological Laboratories) in PBS was administered i.v. on days 0 and 2. Mice were examined daily and scored for disease severity using the standard scale: 0, no clinical signs; 1, limp tail; 2, paraparesis (weakness and incomplete paralysis of one or two hind limbs); 3, paraplegia (complete paralysis of two hind limbs); 4, paraplegia with forelimb weakness or paralysis; and 5, moribund or death. After the onset of EAE, food and water were provided on the cage floor.

Flow cytometry

Cell suspensions were subjected to flow cytometry analyses as previously described (Reiley et al., 2006) using an LSR II flow cytometer (BD).

Isolation and analysis of CNS mononuclear cells

For preparation of CNS mononuclear cells, brains and spinal cords from $MOG_{35–55}$-immunized mice were excised and dissociated for 45 min at 37°C by digestion with 2 mg/ml collagenase IV (Sigma-Aldrich) and 100 µg/ml DNase I (Sigma-Aldrich) in DMEM. Dispersed cells were isolated through a Percoll density gradient and collected on the interface fraction between 37 and 70% Percoll. After intensive washing, suspensions of cells were subjected to flow cytometry.

Intracellular cytokine staining

Mononuclear cells were isolated from spleen, draining lymph nodes, CNS tissues, or tumor tissues of the indicated mice, stimulated in vitro with peptide antigens or PMA plus ionomycin in the presence of monensin, and then subjected to intracellular cytokine staining to detect T cells producing IFN-γ and IL-17. Cells derived from EAE-induced mice were stimulated with the MOG_{35-55} peptide (MEVGWYRSP FSRVVHLYRNGK) for 16 h (monensin added in the last 4 h); cells derived from mice challenged with OVA-expressing tumor cells were stimulated for 16 h (monensin added in the last 4 h) with the MHC I–restricted $OVA_{257–264}$ peptide (SIINFEKL) for analysis of $CD8^+$ T cells or the MHC II–restricted $OVA_{323–339}$ peptide (ISQAVHAAHAEINEAGR) for analysis of $CD4^+$ T cells; and cells derived from other tumor-bearing mice were stimulated for 4 h with PMA plus ionomycin in the presence of monensin. After permeabilization and fixation, the cells were stained with the indicated antibodies and subjected to flow cytometry analyses.

Generation of BMDCs

Bone marrow cells isolated from WT and *Tbk1*-DKO mice were cultured for 7 d in RPMI 1640 medium containing 10% FBS supplemented with 10 ng/ml GM-CSF. The differentiated BMDCs were stained with Pacific blue–conjugated anti-CD11c and isolated by flow cytometry.

Isolation of splenic DCs

Splenic DCs were isolated essentially as described previously (Tavernier et al., 2015). In brief, spleens from WT or *Tbk1*-DKO mice were digested with 0.05% collagenase D (Sigma-Aldrich) and 100 µg/ml DNase I (Sigma-Aldrich) in RPMI 1640 medium for 30 min at 37°C. The cell suspension was spun down and resuspended in a red blood cell

lysis buffer (Sigma-Aldrich) to remove red blood cells. For enrichment of DCs, the cell suspension was stained with anti-CD3 FITC and anti-CD19 FITC antibodies and then incubated with anti-FITC microbeads to eliminate non-DCs by passing through magnetic-activated cell-sorting LD columns (Miltenyi Biotec). The effluent cells (DCs) were stained with anti-CD11c Pacific blue antibody and further purified by flow cytometric cell sorting using a FACSAria II flow cytometer (BD).

In vitro T cell activation assay

Splenic DCs isolated from WT and *Tbk1*-DKO mice were incubated with 10 μg/ml $OVA_{323–339}$ in the presence of 100 ng/ml LPS for 6 h and then washed three times with fresh medium. The pretreated DCs (2×10^3) were incubated with 2×10^5 CFSE-labeled naive OTII $CD4^+$ T cells ($CD44^{lo}CD62L^{hi}$) for 72 h and then subjected to flow cytometric analysis to measure the proliferation of OTII T cells based on CFSE dilution.

Tumor models

B16-F10 and B16-OVA (B16-expressing OVA) melanoma cells were cultured in DMEM supplemented with 10% FBS; EL4 and E.G7-OVA cells (a derivative of EL4 cells expressing OVA) were maintained in RPMI 1640 medium supplemented with 10% FBS. These tumor cells were injected s.c. into 8-wk-old WT and *Tbk1*-DKO mice (5×10^5 for B16 and B16-OVA cells and 10^6 for EL-4 and E.G7-OVA cells). The challenged mice were monitored for tumor growth, and the tumor size was expressed as tumor area. To minimize individual variations, age- and sex-matched, mostly littermate, WT, and *Tbk1*-DKO mice were used.

In tumor models involving DC-based therapy, B16-OVA tumor-bearing WT mice (day 7 after tumor cell inoculation) were injected via tail vein with WT or *Tbk1*-DKO BMDCs pulsed with 10 μg/ml OVA overnight and matured with 100 ng/ml LPS for 6 h. Tumor growth was monitored every other day. For analyzing DC homing properties, the OVA-pulsed and LPS-matured WT and *Tbk1*-DKO BMDCs were labeled with 1 μM CFSE and efluor450 (Thermo Fisher Scientific), respectively, washed three times, and then adoptively transferred as a 1:1 ratio mixture into the B16-OVA tumor-bearing WT mice. After 18 h, flow cytometry was performed to track the migration of WT and DKO DCs to the spleen, draining lymph nodes, and tumors.

RNA-sequencing analysis

Fresh splenic DCs were isolated from young WT and *Tbk1*-DKO mice (6–8 wk old), used for total RNA isolation with TRIzol (Invitrogen), and subjected to RNA-sequencing analysis. RNA sequencing was performed by the MD Anderson Cancer Center Sequencing and Microarray Facility using an Illumina sequencer. The raw reads were aligned to the mm10 reference genome (build mm10), using Tophat2 RNASeq alignment software. The mapping rate was 70% overall across all the samples in the dataset. HTseq-Count was used to quantify the gene expression counts from Tophat2 alignment files. Differential expression analysis was performed on the count data using R package DESeq2. P-values obtained from multiple binomial tests were adjusted using false discovery rate (Benjamini-Hochberg). Significant genes are defined by a Benjamini-Hochberg corrected p-value of cut-off of 0.05 and fold-change of at least two. RNA-sequencing data were deposited to Gene Expression Omnibus under accession number GSE94543.

qRT-PCR

Real-time qRT-PCR was performed as previously described (Chang et al., 2009) using gene-specific primer sets (Table 1). Gene expression was assessed in triplicate and normalized to a reference gene, *Actβ*.

Table 1. **Gene-specific primers used for quantitative PCR**

Gene	Forward primer (5′–3′)	Reverse primer (5′–3′)
Ifna	TGACCTCAAAGCCTGTGTGATG	AAGTATTTCCTCACAGCCAGCAG
Ifnb	AGCTCCAAGAAAGGACGAACAT	GCCCTGTAGGTGAGGTTGATCT
Irf7	CAGCGAGTGCTGTTTGGAGAC	AAGTTCGTACACCTTATGCGG
Irf1	CCCACAGAAGAGCATAGCAC	AGCAGTTCTTTGGGAATAGG
Actin	CGTGAAAAGATGACCCAGATCA	CACAGCCTGGATGGCTACGT
Ifi202b	CCGGGAAACACCATTGCTTT	GGCTCTTCACCTCAGACACG
Slfn8	CCCAGATTTCTCACGCCAGT	GGATGCTGCATGGAGGGTTA
Oas2	TTTACCCCCAAAGTACGCCC	ATGCAGAGCTGCCGGTATTT
Oas3	CCTCAGGAGTCCTTGTGCAG	GAACAGCAAGGTGGCCTTTG
Il10	CCAGAGCCACATGCTCCTAGA	GGTCCTTTGTTTGAAAGAAAGTCTTC
Il6	TGAACAACGATGATGCACTTGC	GCTATGGTACTCCAGAAGACC
Tnf	CATCTTCTCAAAATTCGAGTGACAA	CCAGCTGCTCCTCCACTTG
Il23a	CGTATCCAGTGTGAAGATGGTT	CTATCAGGGAGTAGAGCAGGCT
Il12a	ACTAGAGAGACTTCTTCCACAACAA	CACAGGGTCATCATCAAAGAC
Il12b	GGAGACACCAGCAAAACGAT	TCCAGATTCAGACTCCAGGG
Il1b	AAGCCTCGTGCTGTCGGACC	TGAGGCCCAAGGCCACAGGT

Immunoblotting and IP

Total cell protein extracts were prepared in radio-IP assay buffer and subjected to immunoblotting and IP assays as described previously (Chang et al., 2009).

Statistical analysis

One-way ANOVA, where applicable, was performed to determine whether an overall statistically significant change existed before the Student's *t* test to analyze the difference between any two groups. Data are presented as means ± SD. A p-value <0.05 is considered statistically significant.

ACKNOWLEDGMENTS

We thank C. Wang for expression vectors and S. Akira and Taconic for mice. We also thank the personnel from the National Institutes of Health/National Cancer Institute–supported resources (flow cytometry, sequencing, and microarray facility and animal facility) under grant P30CA016672 at the MD Anderson Cancer Center.

This study was supported by grants from the Cancer Prevention and Research Institute of Texas (RP150235) and the National Institutes of Health (GM84459) and partially supported by a seed fund from the Center for Inflammation and Cancer at the MD Anderson Cancer Center, the National Natural Science Foundation of China (81571545), and the Recruitment Program of Global Experts of China.

The authors declare no competing financial interests.

Author contributions: Y. Xiao, Q. Zou, and X. Xie designed and performed the experiments, prepared the figures, and wrote the manuscript. T. Liu, H.S. Li, Z. Jie, J. Jin, H. Hu, X. Cheng, and H. Wang contributed to the performance of the experiments. G. Manyam and L. Zhang contributed to the microarray analysis. I. Marie and D.E. Levy contributed critical reagents. S.S. Watowich was involved in supervision of H.S. Li, and S.-C. Sun supervised the work and wrote the manuscript.

Submitted: 12 September 2016
Revised: 18 December 2016
Accepted: 9 February 2017

REFERENCES

Ahn, J., and G.N. Barber. 2014. Self-DNA, STING-dependent signaling and the origins of autoinflammatory disease. *Curr. Opin. Immunol.* 31:121–126. http://dx.doi.org/10.1016/j.coi.2014.10.009

Anguille, S., E.L. Smits, E. Lion, V.F. van Tendeloo, and Z.N. Berneman. 2014. Clinical use of dendritic cells for cancer therapy. *Lancet Oncol.* 15:e257–e267. http://dx.doi.org/10.1016/S1470-2045(13)70585-0

Baratin, M., C. Foray, O. Demaria, M. Habbeddine, E. Pollet, J. Maurizio, C. Verthuy, S. Davanture, H. Azukizawa, A. Flores-Langarica, et al. 2015. Homeostatic NF-κB signaling in steady-state migratory dendritic cells regulates immune homeostasis and tolerance. *Immunity.* 42:627–639. http://dx.doi.org/10.1016/j.immuni.2015.03.003

Bonnard, M., C. Mirtsos, S. Suzuki, K. Graham, J. Huang, M. Ng, A. Itié, A. Wakeham, A. Shahinian, W.J. Henzel, et al. 2000. Deficiency of T2K leads to apoptotic liver degeneration and impaired NF-κB-dependent gene transcription. *EMBO J.* 19:4976–4985. http://dx.doi.org/10.1093/emboj/19.18.4976

Chang, M., W. Jin, and S.C. Sun. 2009. Peli1 facilitates TRIF-dependent Toll-like receptor signaling and proinflammatory cytokine production. *Nat. Immunol.* 10:1089–1095. http://dx.doi.org/10.1038/ni.1777

Cheng, F., H.W. Wang, A. Cuenca, M. Huang, T. Ghansah, J. Brayer, W.G. Kerr, K. Takeda, S. Akira, S.P. Schoenberger, et al. 2003. A critical role for Stat3 signaling in immune tolerance. *Immunity.* 19:425–436. http://dx.doi.org/10.1016/S1074-7613(03)00232-2

Clark, K., L. Plater, M. Peggie, and P. Cohen. 2009. Use of the pharmacological inhibitor BX795 to study the regulation and physiological roles of TBK1 and IκB kinase epsilon: a distinct upstream kinase mediates Ser-172 phosphorylation and activation. *J. Biol. Chem.* 284:14136–14146. http://dx.doi.org/10.1074/jbc.M109.000414

Dalod, M., R. Chelbi, B. Malissen, and T. Lawrence. 2014. Dendritic cell maturation: functional specialization through signaling specificity and transcriptional programming. *EMBO J.* 33:1104–1116. http://dx.doi.org/10.1002/embj.201488027

Dhodapkar, M.V., R.M. Steinman, J. Krasovsky, C. Munz, and N. Bhardwaj. 2001. Antigen-specific inhibition of effector T cell function in humans after injection of immature dendritic cells. *J. Exp. Med.* 193:233–238. http://dx.doi.org/10.1084/jem.193.2.233

Dudek, A.M., S. Martin, A.D. Garg, and P. Agostinis. 2013. Immature, semi-mature, and fully mature dendritic cells: toward a DC-cancer cells interface that augments anticancer immunity. *Front. Immunol.* 4:438. http://dx.doi.org/10.3389/fimmu.2013.00438

Fitzgerald, K.A., S.M. McWhirter, K.L. Faia, D.C. Rowe, E. Latz, D.T. Golenbock, A.J. Coyle, S.M. Liao, and T. Maniatis. 2003. IKKε and TBK1 are essential components of the IRF3 signaling pathway. *Nat. Immunol.* 4:491–496. http://dx.doi.org/10.1038/ni921

Fuertes, M.B., S.R. Woo, B. Burnett, Y.X. Fu, and T.F. Gajewski. 2013. Type I interferon response and innate immune sensing of cancer. *Trends Immunol.* 34:67–73. http://dx.doi.org/10.1016/j.it.2012.10.004

Hall, J.C., and A. Rosen. 2010. Type I interferons: crucial participants in disease amplification in autoimmunity. *Nat. Rev. Rheumatol.* 6:40–49. http://dx.doi.org/10.1038/nrrheum.2009.237

Hammer, G.E., and A. Ma. 2013. Molecular control of steady-state dendritic cell maturation and immune homeostasis. *Annu. Rev. Immunol.* 31:743–791. http://dx.doi.org/10.1146/annurev-immunol-020711-074929

Hawiger, D., K. Inaba, Y. Dorsett, M. Guo, K. Mahnke, M. Rivera, J.V. Ravetch, R.M. Steinman, and M.C. Nussenzweig. 2001. Dendritic cells induce peripheral T cell unresponsiveness under steady state conditions in vivo. *J. Exp. Med.* 194:769–780. http://dx.doi.org/10.1084/jem.194.6.769

Hemmi, H., O. Takeuchi, S. Sato, M. Yamamoto, T. Kaisho, H. Sanjo, T. Kawai, K. Hoshino, K. Takeda, and S. Akira. 2004. The roles of two IκB kinase-related kinases in lipopolysaccharide and double stranded RNA signaling and viral infection. *J. Exp. Med.* 199:1641–1650. http://dx.doi.org/10.1084/jem.20040520

Hiscott, J. 2007. Triggering the innate antiviral response through IRF-3 activation. *J. Biol. Chem.* 282:15325–15329. http://dx.doi.org/10.1074/jbc.R700002200

Ho, H.H., and L.B. Ivashkiv. 2010. Downregulation of Friend leukemia virus integration 1 as a feedback mechanism that restrains lipopolysaccharide induction of matrix metalloproteases and interleukin-10 in human macrophages. *J. Interferon Cytokine Res.* 30:893–900. http://dx.doi.org/10.1089/jir.2010.0046

Ivashkiv, L.B., and L.T. Donlin. 2014. Regulation of type I interferon responses. *Nat. Rev. Immunol.* 14:36–49. http://dx.doi.org/10.1038/nri3581

Jin, J., Y. Xiao, J.H. Chang, J. Yu, H. Hu, R. Starr, G.C. Brittain, M. Chang, X. Cheng, and S.C. Sun. 2012. The kinase TBK1 controls IgA class switching by negatively regulating noncanonical NF-κB signaling. *Nat. Immunol.* 13:1101–1109. http://dx.doi.org/10.1038/ni.2423

Li, H.S., C. Liu, Y. Xiao, F. Chu, X. Liang, W. Peng, J. Hu, S.S. Neelapu, S.-C. Sun, P. Hwu, and S.S. Watowich. 2016. Bypassing STAT3-mediated inhibition of the transcriptional regulator ID2 improves the antitumor efficacy of dendritic cells. *Sci. Signal.* 9:ra94. http://dx.doi.org/10.1126/scisignal.aaf3957

Liu, S., X. Cai, J. Wu, Q. Cong, X. Chen, T. Li, F. Du, J. Ren, Y.T. Wu, N.V. Grishin, and Z.J. Chen. 2015. Phosphorylation of innate immune adaptor proteins MAVS, STING, and TRIF induces IRF3 activation. *Science.* 347:aaa2630. http://dx.doi.org/10.1126/science.aaa2630

Mahnke, K., E. Schmitt, L. Bonifaz, A.H. Enk, and H. Jonuleit. 2002. Immature, but not inactive: the tolerogenic function of immature dendritic cells. *Immunol. Cell Biol.* 80:477–483. http://dx.doi.org/10.1046/j.1440-1711.2002.01115.x

Maueröder, C., L.E. Munoz, R.A. Chaurio, M. Herrmann, G. Schett, and C. Berens. 2014. Tumor immunotherapy: lessons from autoimmunity. *Front. Immunol.* 5:212. http://dx.doi.org/10.3389/fimmu.2014.00212

Mayer, C.T., L. Berod, and T. Sparwasser. 2012. Layers of dendritic cell-mediated T cell tolerance, their regulation and the prevention of autoimmunity. *Front. Immunol.* 3:183. http://dx.doi.org/10.3389/fimmu.2012.00183

McWhirter, S.M., K.A. Fitzgerald, J. Rosains, D.C. Rowe, D.T. Golenbock, and T. Maniatis. 2004. IFN-regulatory factor 3-dependent gene expression is defective in *Tbk1*-deficient mouse embryonic fibroblasts. *Proc. Natl. Acad. Sci. USA.* 101:233–238. http://dx.doi.org/10.1073/pnas.2237236100

Melillo, J.A., L. Song, G. Bhagat, A.B. Blazquez, C.R. Plumlee, C. Lee, C. Berin, B. Reizis, and C. Schindler. 2010. Dendritic cell (DC)-specific targeting reveals Stat3 as a negative regulator of DC function. *J. Immunol.* 184:2638–2645. http://dx.doi.org/10.4049/jimmunol.0902960

Ng, J., and D. Cantrell. 1997. STAT3 is a serine kinase target in T lymphocytes. Interleukin 2 and T cell antigen receptor signals converge upon serine 727. *J. Biol. Chem.* 272:24542–24549. http://dx.doi.org/10.1074/jbc.272.39.24542

O'Shea, N.R., T.S. Chew, J. Dunne, R. Marnane, B. Nedjat-Shokouhi, P.J. Smith, S.L. Bloom, A.M. Smith, and A.W. Segal. 2016. Critical role of the disintegrin metalloprotease ADAM-like Decysin-1 [ADAMDEC1] for intestinal immunity and inflammation. *J. Crohn's Colitis.* 10:1417–1427. http://dx.doi.org/10.1093/ecco-jcc/jjw111

Perry, A.K., E.K. Chow, J.B. Goodnough, W.C. Yeh, and G. Cheng. 2004. Differential requirement for TANK-binding kinase-1 in type I interferon responses to toll-like receptor activation and viral infection. *J. Exp. Med.* 199:1651–1658. http://dx.doi.org/10.1084/jem.20040528

Reiley, W.W., M. Zhang, W. Jin, M. Losiewicz, K.B. Donohue, C.C. Norbury, and S.C. Sun. 2006. Regulation of T cell development by the deubiquitinating enzyme CYLD. *Nat. Immunol.* 7:411–417. http://dx.doi.org/10.1038/ni1315

Seya, T., H. Shime, T. Ebihara, H. Oshiumi, and M. Matsumoto. 2010. Pattern recognition receptors of innate immunity and their application to tumor immunotherapy. *Cancer Sci.* 101:313–320. http://dx.doi.org/10.1111/j.1349-7006.2009.01442.x

Sharma, P., K. Wagner, J.D. Wolchok, and J.P. Allison. 2011. Novel cancer immunotherapy agents with survival benefit: recent successes and next steps. *Nat. Rev. Cancer.* 11:805–812. http://dx.doi.org/10.1038/nrc3153

Sharma, S., B.R. tenOever, N. Grandvaux, G.P. Zhou, R. Lin, and J. Hiscott. 2003. Triggering the interferon antiviral response through an IKK-related pathway. *Science.* 300:1148–1151. http://dx.doi.org/10.1126/science.1081315

Shen, Y., K. Schlessinger, X. Zhu, E. Meffre, F. Quimby, D.E. Levy, and J.E. Darnell Jr. 2004. Essential role of STAT3 in postnatal survival and growth revealed by mice lacking STAT3 serine 727 phosphorylation. *Mol. Cell. Biol.* 24:407–419. http://dx.doi.org/10.1128/MCB.24.1.407-419.2004

Simmons, S.B., E.R. Pierson, S.Y. Lee, and J.M. Goverman. 2013. Modeling the heterogeneity of multiple sclerosis in animals. *Trends Immunol.* 34:410–422. http://dx.doi.org/10.1016/j.it.2013.04.006

Steinman, R.M., D. Hawiger, and M.C. Nussenzweig. 2003. Tolerogenic dendritic cells. *Annu. Rev. Immunol.* 21:685–711. http://dx.doi.org/10.1146/annurev.immunol.21.120601.141040

Takeda, K., T. Kaisho, N. Yoshida, J. Takeda, T. Kishimoto, and S. Akira. 1998. Stat3 activation is responsible for IL-6-dependent T cell proliferation through preventing apoptosis: generation and characterization of T cell-specific Stat3-deficient mice. *J. Immunol.* 161:4652–4660.

Tavernier, S.J., F. Osorio, S. Janssens, and B.N. Lambrecht. 2015. Isolation of splenic dendritic cells using fluorescence-activated cell sorting. *Bio Protoc.* 5:e1415. http://dx.doi.org/10.21769/BioProtoc.1415

Toomer, K.H., and Z. Chen. 2014. Autoimmunity as a double agent in tumor killing and cancer promotion. *Front. Immunol.* 5:116. http://dx.doi.org/10.3389/fimmu.2014.00116

van Vliet, S.J., J. den Dunnen, S.I. Gringhuis, T.B. Geijtenbeek, and Y. van Kooyk. 2007. Innate signaling and regulation of dendritic cell immunity. *Curr. Opin. Immunol.* 19:435–440. http://dx.doi.org/10.1016/j.coi.2007.05.006

Wang, W.B., D.E. Levy, and C.K. Lee. 2011. STAT3 negatively regulates type I IFN-mediated antiviral response. *J. Immunol.* 187:2578–2585. http://dx.doi.org/10.4049/jimmunol.1004128

Woo, S.R., M.B. Fuertes, L. Corrales, S. Spranger, M.J. Furdyna, M.Y.K. Leung, R. Duggan, Y. Wang, G.N. Barber, K.A. Fitzgerald, et al. 2014. STING-dependent cytosolic DNA sensing mediates innate immune recognition of immunogenic tumors. *Immunity.* 41:830–842. http://dx.doi.org/10.1016/j.immuni.2014.10.017

Yu, J., X. Zhou, M. Chang, M. Nakaya, J.H. Chang, Y. Xiao, J.W. Lindsey, S. Dorta-Estremera, W. Cao, A. Zal, et al. 2015. Regulation of T-cell activation and migration by the kinase TBK1 during neuroinflammation. *Nat. Commun.* 6:6074. http://dx.doi.org/10.1038/ncomms7074

Zou, W., J.D. Wolchok, and L. Chen. 2016. PD-L1 (B7-H1) and PD-1 pathway blockade for cancer therapy: Mechanisms, response biomarkers, and combinations. *Sci. Transl. Med.* 8:328rv4. http://dx.doi.org/10.1126/scitranslmed.aad7118